Intensity Coding in Electric Hearing: Effects of Electrode Configurations and Stimulation Waveforms

Tiffany Elise H. Chua,[1] Mark Bachman,[1,2] and Fan-Gang Zeng[1,3,4,5]

Objectives: Current cochlear implants typically stimulate the auditory nerve with biphasic pulses and monopolar electrode configurations. Tripolar stimulation can increase spatial selectivity and potentially improve place pitch related perception but requires higher current levels to elicit the same loudness as monopolar stimulation. The present study combined delayed pseudomonophonasic pulses, which produce lower thresholds, with tripolar stimulation in an attempt to solve the power-performance tradeoff problem.

Design: The present study systematically measured thresholds, dynamic range, loudness growth, and intensity discrimination using either biphasic or delayed pseudomonophonasic pulses under both monopolar and tripolar stimulation. Participants were five Clarion cochlear implant users. For each subject, data from apical, middle, and basal electrode positions were collected when possible.

Results: Compared with biphasic pulses, delayed pseudomonophonasic pulses increased the dynamic range by lowering thresholds while maintaining comparable maximum allowable levels under both electrode configurations. However, delayed pseudomonophonasic pulses did not change the shape of loudness growth function and actually increased intensity discrimination limens, especially at lower current levels.

Conclusions: The present results indicate that delayed pseudomonophonasic pulses coupled with tripolar stimulation cannot provide significant power savings nor can it increase the functional dynamic range. Whether this combined stimulation could improve functional spectral resolution remains to be seen.

(Ear & Hearing 2011;32;1–●)

INTRODUCTION

Cochlear implants (CIs) can be driven in several modes. In traditional monopolar (Mono) stimulation mode, the stimulating electrode is located inside the scala tympani while the return electrode is located outside, producing a broad excitation pattern in response to stimulation. The low spectral resolution associated with the use of broad Mono stimulation is one reason for relatively poor performance in CI users under challenging listening conditions. To increase spectral resolution, CIs can be driven in tripolar (Tri) stimulation mode (Ifukube & White 1987), where the return electrodes are located adjacent to or near the stimulating electrode, producing narrower excitation patterns. Evidence for sharper excitation patterns in Tri stimulation can be found in physical models (Jolly et al. 1996), recordings from populations of auditory nerve fibers (van den Honert & Stypulkowski 1987), and recordings from the inferior colliculus and auditory cortex (Bierer & Middlebrooks 2002; Snyder et al. 2004, 2008). However, clinical studies implementing Tri stimulation have shown limited success because of the high current requirements with Tri stimulation, often reaching the compliance voltage of the CI device (Mens & Berenstein 2005; Litvak et al. 2007; Bonham & Litvak 2008). Techniques such as partial Tri stimulation (Kral et al. 1998; Bonham & Litvak 2008), where current is partly returned to the adjacent electrodes and partly to the remote ground electrode, can reduce the thresholds required for Tri stimulation by trading off a small degree of spectral resolution and increasing the traversal current component reaching the nerve fibers.

There have also been a number of different approaches used to lower current requirements for electrical stimulation. First, high-rate (>2000 Hz) pulses, which produce pseudospontaneous spike trains with statistical properties similar to spontaneous activity in normal spiral ganglion cells (Rubinstein et al. 1999), can reduce thresholds and increase dynamic range (Hong et al. 2003). Second, Gaussian noise added to the input signals, which presumably makes electric and acoustic responses more similar, has been shown to increase dynamic range by reducing thresholds and increasing maximum allowable levels (Zeng et al. 2000; Morse et al. 2007). Third, different from standard charge-balanced biphasic (BP) pulses, alternative stimulus waveforms such as delayed pseudomonophasic (DP) pulses (van Wieringen et al. 2005; Macherey et al. 2006) and triphasic pulses (Bonnet et al. 2004; Eddington et al. 2004) provide more efficient stimulation to activate the neural tissue. Such efficient stimulus waveforms could also increase the maximum charge density, allowing smaller electrodes to be used in future CI devices (Brummer & Turner 1977).

Typically, CIs provide electric stimulation using BP pulses, in which the second phase is equal in duration as the first phase but opposite in amplitude. This assures charge balance to reverse faradaic reactions that mediate charge injection. However, due to charge integration in the neural membrane, charge injection by the initial phase is almost immediately counteracted by the second phase (van den Honert & Mortimer 1979). Compared with using monophasic pulses, which consist of a single phase, higher current levels are needed to elicit thresholds using BP pulses. Alternative waveforms have been proposed to provide more efficient stimulation to activate neural tissue. Among different alternative stimulus waveforms investigated using Mono stimulation, DP pulses (Carlyon et al. 2005) led to the largest threshold reduction: a 16-dB drop compared with standard BP pulses (Macherey et al. 2006). DP pulses approach the efficiency of monophasic pulses by adding a gap between pulses to delay charge recovery and using a low-amplitude second phase to redistribute the charge over a longer phase duration. These manipulations prevent the second phase from suppressing the occurrence of an action potential generated by the first phase (Shepherd & Javel 1999). In addition, DP pulses may provide more selective excitation by reducing the lateral peaks generated at higher current levels by

[1]Department of Biomedical Engineering, [2]Electrical and Computer Engineering, [3]Anatomy and Neurophysiology, [4]Cognitive Sciences, and [5]Otolaryngology-Head and Neck Surgery, University of California, Irvine, Irvine, California.

0196/0202/11/3203-0001/0 • Ear & Hearing • Copyright © 2011 by Lippincott Williams & Wilkins • Printed in the U.S.A.

TABLE 1. Subjects' demographic and audiological information

Subject	Age	Duration of Deafness (yrs)	Etiology	Years Implanted	Device	Electrode	Phase Duration (μsecs)	Tri Mode
S1	66	64	Spinal meningitis	3	CII	3	226.4	Tri + 0
						8	226.4	Tri + 0
						13	226.4	Tri + 0
S2	71	65	Unknown	7	CII	3	107.8	Tri + 0
						8	107.8	Tri + 0
						13	107.8	Tri + 0
S3	55	40	Unknown	3	HiRes	3	226.4	Tri + 1
						8	226.4	Tri + 1
S4	49	4	Unknown	3	HiRes	3	226.4	Tri + 0
						8	226.4	Tri + 0
						13	226.4	Tri + 0
S5	52	52	Genetic	6	CII	3	226.4	Tri + 0
						8	107.8	Tri + 0
						13	107.8	Tri + 0

the low-amplitude second phase (Frijns et al. 1996; Jolly et al. 1996).

To our knowledge, the application of more efficient waveforms to Tri stimulation has not been studied. Thus, in the present study, we measured thresholds, maximum allowable levels, and dynamic range to confirm the reduced current requirements using DP pulses with Mono and Tri stimulation (Experiment 1). In addition, we characterized intensity coding by examining loudness growth functions (Experiment 2) and intensity discrimination limens (Experiment 3). Standard BP pulses were used as a control condition.

SUBJECTS AND METHODS

Subjects

Five CI subjects using Advanced Bionics Clarion CII or HiRes90K devices participated. Table 1 lists subjects' demographic and device information as well as electrical stimulation parameters used in the experiments. In subjects for whom maximum allowable levels with Tri stimulation could not be reached within device compliance limits, the spacing between active and reference electrodes was increased by 1 (e.g., S3) and/or the phase duration was increased from 107.78 to 226.34 μsecs (e.g., S1, S3, S4, and S5). Stimulation parameters were sometimes different across electrodes. For example, in S5, maximum allowable levels could be attained with a short 107.8-μsec pulse duration for electrodes 8 and 13 but not for electrode 3. For S3, five of the most basal electrodes in the clinical map were turned off due to vibrotactile percepts. Electrode 13 was not tested. Both Institutional Review Board approval and written informed consent were obtained before data collection. Subjects were compensated for both time and travel expenses.

Stimuli

Stimuli consisted of 500-msec, 100 Hz pulse trains applied to an apical (E3), middle (E8), or basal (E13) electrode. Electrode configuration was either Mono or Tri, and the reference was the case electrode for Mono stimulation. Figure 1a shows the difference in electrode and current source configuration between Mono and Tri stimulation. For Tri stimulation, electrodes adjacent to the center electrode were used (Tri + 0) except for S3 who needed a spacing of 1 electrode (Tri + 1) to reach maximum allowable levels. Figure 1b illus-

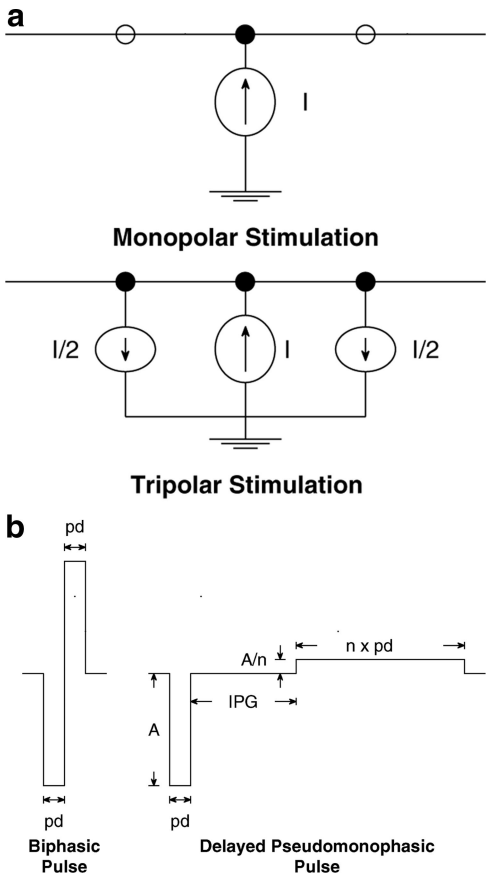

Fig. 1. Electric stimulation modes and pulse waveforms. a, Monopolar versus tripolar stimulation. Current is delivered through the active electrode and returned through the reference electrode(s). Circles along the line represent electrodes along the array. The ground symbol represents a remote electrode, either a ball electrode implanted under the temporalis muscle or a plate electrode located on the receiver-stimulator case. b, Biphasic (BP) versus delayed pseudomonophasic (DP) pulses. The waveform is symmetrical for BP pulses and asymmetrical for DP pulses. Charge balance is maintained.

trates the difference in pulse shape between the standard BP pulse and the DP pulse. The polarity of the leading phase was always cathodic in both pulse shapes. The phase duration was set to 107.78 μsecs for the majority of subjects and to 226.34 μsecs for electrodes in which the subject could not reach a comfortable level with Tri stimulation. For DP pulses, the phase duration of the second phase was set to eight times the phase duration of the first phase, while the amplitude was set to one-eighth of the first phase to maintain charge balance. The interphase gap was 4.7 msecs. A total of four combinations of electrode configuration and pulse shape were used, namely, Mono-BP, Mono-DP, Tri-BP, and Tri-DP. A 100 Hz pulse rate was chosen as previous studies showed that the effect of delaying charge recovery for DP pulses may be greater at low stimulation rates (Carlyon et al. 2005).

Stimuli were generated and presented using the Advanced Bionics Bionic Ear Data Collection System (BEDCS) and custom-made Visual Basic programs that controlled the BEDCS interface. The intensity step sizes were 1, 2, 4, and 8 μA, for current ranging between 0 to 255, 256 to 510, 512 to 1020, and 1024 to 2040 μA respectively. For DP pulses, the step size in each range was effectively multiplied by 8 due to the restriction that the amplitude of the low-amplitude second phase must be one-eighth of the amplitude of the first phase. This may account for the finding that SDs for measurements using DP pulses were larger than standard BP pulses.

Stimulation safety of DP pulses has been discussed in previous studies (Carlyon et al. 2005; Macherey et al. 2006). In a study using earlier Laura implants (van Wieringen et al. 2005), the difference between actual absolute amplitude and requested amplitude due to nonlinear current sources caused a short-term charge imbalance even after applying a correction factor to compensate for this discrepancy. The magnitude of the difference depended on the impedance across two electrodes, but the short-term charge imbalance could be recovered by the blocking capacitor in series with the electrode within a few milliseconds. Current sources in present CI devices exhibit better amplitude linearity so that correction factors are not needed.

The maximum current that can be delivered by the device is also limited by the voltage compliance, which is 8 V in Clarion devices. Part of the voltage is built up across the electrode, which is designed to be <0.9 V, beyond which the "water window" occurs (Brummer & Turner 1977; Robblee & Rose 1990; Merrill et al. 2005; Cogan 2008). The water window refers to the voltage range in which water does not get oxidized or reduced as a side effect of the electrochemical reaction. Beyond this voltage range, the electrolysis of water occurs, causing harmful pH changes and gas formation. The output impedance of the device is not high enough to maintain constant current across a varying load such as the impedance of tissue. Typically, the current source generates a stimulating current from a data source, where the input value can go up to 2048 μA. However, when load impedance is too high, the output current would be limited by (Litvak, personal communication): $I = \frac{(V - 0.9)}{R_a + 0.01 \times \mathrm{PD}}$, where V is the nominal compliance voltage of 8 V, R_a is the access impedance of the electrode or resistive part of impedance measured using SoundWave® in kΩ, I is the current in mA, and PD is the pulse duration in μsecs. The term $0.01 \times \mathrm{PD} \times I$ accounts for the contribution of the built-in capacitor. Typically, R_a ranges from 1 to 10 kΩ. For a pulse duration PD of 108 μsecs and with $R_a = 1$ kΩ, maximum current I allowed before the device reaches compliance is as high as 3414 μA. With $R_a = 10$ kΩ, maximum current I is 641 μA. For a pulse duration PD of 226 μsecs, and with $R_a = 1$ kΩ and $R_a = 10$ kΩ, the maximum current I drops slightly to 2178 and 579 μA, respectively. The most limited case in this study (S5, E13) had an R_a of 9.9 kΩ, resulting in maximum current I of 717 μA or 56.48 dB re 1 μA. Thus, if I is >2048 μA, the full output current range can be delivered by the device, and if I is <2048 μA, the output current is limited by the compliance voltage.

Procedures

Experiment 1—Thresholds and Maximum Allowable Levels • Thresholds were measured using a two-down, one-up, three-interval forced-choice (3IFC), adaptive procedure. Initial values were set to very soft or soft levels. Step size was set to four or eight current steps for the first two reversals and one current step for the succeeding reversals. One current step was equivalent to 1, 2, 4, and 8 μA for current ranging between 0 to 255, 256 to 510, 512 to 1020, and 1024 to 2040 μA, respectively. The average of the last six of nine reversals was taken as threshold. Each threshold was measured twice, or thrice if the first two measures varied by >3 μA. Maximum allowable levels (MALs) were measured using the method of adjustments. Subjects controlled a custom interface with volume up and volume down buttons until maximum comfort level was reached. A stimulus was delivered on each press of a volume control button and could be replayed by clicking on another button. Subjects were instructed to proceed carefully when comfort levels were reached. All four combinations of stimulation mode and pulse shape were available simultaneously on screen for the subject to compare in any order at any time. On a given experiment run, subjects worked on obtaining the MAL for one of the four conditions. Subjects were able to refer to MALs selected for the other three conditions if already selected and adjust present or past selections. Data were obtained from electrodes 3 (apical), 8 (middle), and 13 (basal), with four conditions (Mono/BP, Mono/DP, Tri/BP, and Tri/DP) per electrode. The order of test conditions and electrodes was not systematically randomized.

Experiment 2—Loudness Growth Functions • Loudness growth functions were measured using magnitude estimation. Subjects were instructed to judge the loudness of the stimuli by assigning a number from 0 to 100 and to judge each stimulus presentation independently. For each condition, loudness estimates were obtained thrice at six evenly distributed levels at 0, 20, 40, 60, 80, and 100% of the dynamic range in μA, defined as the difference between threshold and MAL obtained from Experiment 1. Data were obtained from electrodes 3, 8, and 13 used in experiment 1. Each run presented stimuli at a single electrode, for a total of 4 conditions per run × 6 levels per condition × 3 trials per level = 72 trials per run. Stimuli were quasirandomized over all conditions, so that no consecutive presentations were the same, and the first stimulus was neither the minimum nor the maximum level. One set of practice stimuli, containing one sample for each of the 24 possible stimuli, was provided before each run to familiarize the subject with the stimuli. Responses from practice runs were discarded.

TABLE 2. Loudness growth models and derived rates of loudness growth

Model	Equation	Rate of Loudness Growth
Linear function	$y = ax + b$	$y' = a$
Exponential function	$y = ae^{bx}$	$y' = abe^{bx}$
Power function	$y = ax^{b}$	$y' = abx^{b-1}$

Experiment 3—Just Noticeable Differences in Current Amplitude • Just noticeable differences (JNDs) in current amplitude were measured using a two-down, one-up, 3IFC adaptive procedure. The initial step size was set to one, two, or four current steps for the first two reversals and one current step for the succeeding reversals. The average of the last six of nine reversals was reported. JNDs at 20, 40, 60, and 80% of the dynamic range in μA were measured twice or thrice, if time permitted, per condition per electrode. This corresponded to different values of percent dynamic range in dB depending on the subject's threshold and MAL.

Data Analysis

Best-Fit Loudness Growth Functions and Rates of Loudness Growth • To account for differences in loudness scale across subjects and within subjects across different experiment runs, loudness ratings were normalized by the maximum number assigned to any stimuli within a single run. Loudness growth was modeled with three different functions—linear, exponential, and power functions. Table 2 lists the equations for different loudness models. Each model uses one parameter to describe the rate of loudness growth and one or two parameters to shift or scale the function along the x or y axis. Best-fit models for each loudness growth curve were determined by computing Akaike weights for three candidate models and choosing the model with the highest weight. The Akaike weights, derived from Akaike information criterion (AIC) values, represent the probability that the model is correct given the underlying data (Akaike 1978, 1979; Bozdogan 1987; Burnham & Anderson 2002; Wagenmakers & Farrell 2004). The method accounts for both accuracy and parsimony of the model, and its main advantage is that it is easy to compute and interpret. However, the method is subject to sampling variability, so a different sample could result in a different set of weights for the candidate models. It should be noted that in this experiment the evidence ratio or relative likelihoods of the best-fit model to the next best-fit model was <10 in most cases and <2 in half of the cases. Slopes of loudness growth functions were calculated by evaluating the derivatives of fitted curves at 20, 40, 60, and 80% of dynamic range. The Akaike-weighted average from three candidate models was taken as the averaged slope to represent the rate of loudness growth.

Weber Fractions in dB and Number of Discriminable Steps

Weber fractions in dB were computed by $10\log\left(\frac{\Delta I}{I}\right)$, where $\frac{\Delta I}{I} = \frac{\Delta A^2}{A^2} + \frac{2\Delta A}{A}$. ΔA is the JND in current amplitude at the specified current level A in μA (Pfingst et al. 1983). The formula reflects the fact that the power or intensity of a signal added to the pedestal is the squared sum of the amplitudes of the signal and pedestal (Grantham & Yost 1982). Percent dynamic range in dB was calculated by $\frac{20\log A - 20\log A_{\mathrm{THS}}}{20\log A_{\mathrm{MAL}} - 20\log A_{\mathrm{THS}}}$, where A_{THS} was the current amplitude at threshold (THS) and A_{MAL} was the current amplitude at maximum allowable level (MAL). For each condition, empirical Weber functions were derived by fitting data to the equation $\mathrm{Wf_{db}} = a(\%\mathrm{DR_{db}}) + b$, similar to functions that describe intensity discrimination in normal hearing, but with sensation level normalized by dynamic range to account for the compressed intensity dimension in electric hearing (Nelson et al. 1996). The parameter a is the slope of the Weber function, describing the change in Weber fraction per unit change in percent dynamic range, and the parameter b is the sensitivity constant, describing the size of the Weber fraction at threshold. The F-test comparing the Weber function and a simpler model $\mathrm{Wf_{db}} = b$, where the size of the Weber fraction does not change with percent dynamic range, was also computed to determine whether slopes of Weber functions were significantly different from zero (Nelson et al. 1996).

The number of discriminable steps over the dynamic range was quantified by dividing the full 100% dynamic range by the average intensity JND expressed as a percentage of the dynamic range (Kreft et al. 2004):

$$\text{No. of steps} = \frac{100\%}{\Delta I_{\%\mathrm{DR\_AVG}}}$$

$$\Delta I_{\%\mathrm{DR\_AVG}} = \frac{\Delta I_{\mathrm{dB\_AVG}}}{\mathrm{DR_{dB}}} \times 100$$

The average intensity JND was calculated by first deriving the expression for ΔI_{db} as a function of $\%\mathrm{DR_{db}}$, and then using the mean value theorem to compute $\Delta I_{\mathrm{db\_AVG}}$. The parameters a and b below are Weber function parameters.

$$\Delta I_{\mathrm{dB}} = 10\log\frac{I + \Delta I}{I} = 10\log(1 + \mathrm{Wf})$$

$$= 10\log\left(1 + 10^{\frac{1}{10}a(\%\mathrm{DR_{dB}})+b}\right)$$

$$\Delta I_{\mathrm{dB\_AVG}} = \frac{1}{100}\int_{0}^{100} \Delta I_{\mathrm{dB}}(\%\mathrm{DR_{dB}})\,d(\%\mathrm{DR_{dB}})$$

RESULTS

Experiment 1—Thresholds and Maximum Allowable Levels

The purpose of this experiment was to replicate previous studies on the effect of DP pulses using Mono stimulation and assess the feasibility of using DP pulses to reduce power requirements of Tri stimulation. Standard BP pulses were used as control. Data from this experiment were also needed for subsequent loudness growth and intensity discrimination experiments.

Figure 2 shows results from five subjects (top five rows) as well as average data (bottom panels). Bars represent the

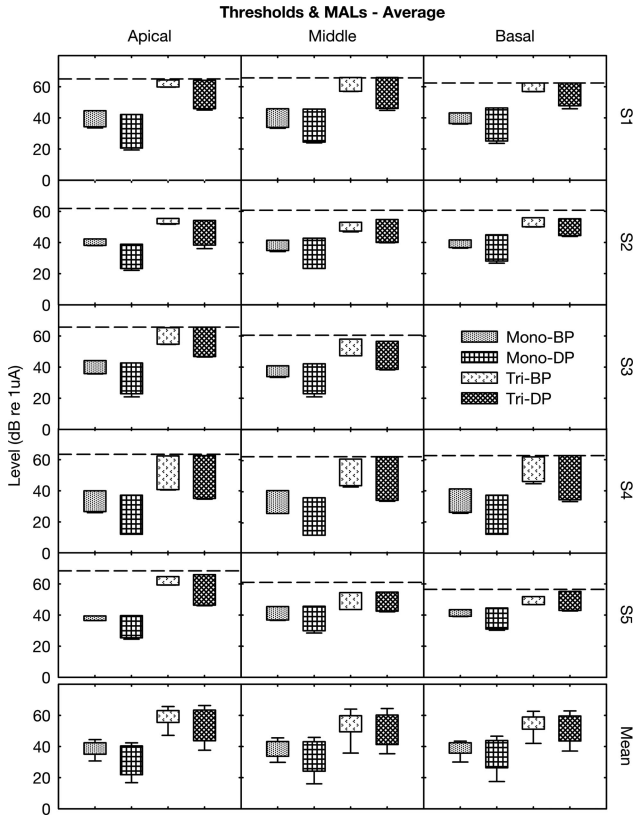

Fig. 2. Thresholds and maximum allowable levels for Mono-BP (dotted bars), Mono-DP (crosshatched bars), Tri-BP (speckled bars), and Tri-DP (diagonally crosshatched bars) stimuli. Bars span the dynamic range from threshold to MAL and error bars mark 1 SD.

dynamic range spanning thresholds to MALs. Error bars mark 1 SD. No data were collected from electrode 13 of S3 due to vibrotactile percepts associated with this electrode. To account for missing data, two sets of analysis of variance (ANOVA) were performed—one with apical and middle electrodes in five subjects and one with apical, middle, and basal electrodes in four subjects. Factors in ANOVA included electrode position (E3 and E8 or E3, E8 and E13), stimulation mode (Mono and Tri), and pulse shape (BP and DP). Despite different degrees of freedom and F-values, both ANOVA sets produced the same conclusions. Hence, only the p value is reported below.

Across electrodes, thresholds and MALs were similar ($p > 0.05$). Collapsed across all conditions, average thresholds for electrodes 3, 8, and 13 were 46.2, 41.5, and 43.4 dB re 1 μA, and average MALs were 57.9, 55.1, and 54.5 dB re 1 μA, respectively. These dB re 1 μA values corresponded to average thresholds of 203, 119, and 148 μA and average MALs of 782, 568, and 532 μA, respectively. For Mono stimulation, average thresholds for electrodes 3, 8, and 13 were 30.8, 30.2, and 32.2 dB re 1 μA, and average MALs were 41.4, 43.1, and 43.1 dB re 1 μA, respectively. For Tri stimulation, average thresholds for electrodes 3, 8, and 13 were 51.4, 46.2, and 48.1 dB re 1 μA, and average MALs were 63.2, 60.0, and 59.3 dB re 1 μA, respectively.

On average, Tri stimulation produced 17.9 dB higher thresholds ($p < 0.01$) as well as 18.5 dB higher MALs than Mono stimulation ($p < 0.01$). The parallel change in thresholds and MALs produced the same dynamic range of about 12 dB for both Mono and Tri stimulation. Note that, due to high current levels in Tri stimulation, the MALs approached the calculated voltage compliance limit in most cases (dashed lines), possibly underestimating MALs.

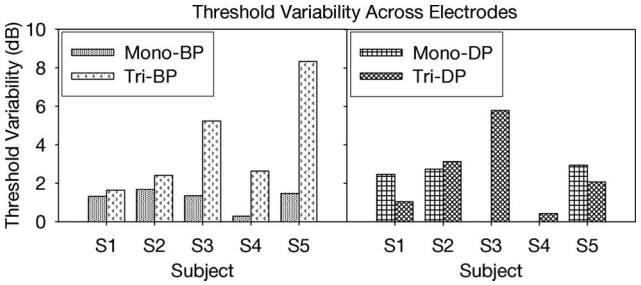

Fig. 3. Threshold variability across electrodes in five subjects for Mono-BP (dotted bars), Mono-DP (crosshatched bars), Tri-BP (speckled bars), and Tri-DP (diagonally crosshatched bars) stimuli.

Consistent with data reported by Macherey et al. (2006), DP pulses produced significantly lower thresholds compared with BP pulses ($p < 0.01$), dropping by 9.7 dB re 1 μA on the average, but produced strikingly similar MALs compared with BP pulses (0.3 dB difference on the grand average, $p > 0.05$). Therefore, the increased dynamic range with the DP waveform was solely a result of the lowered threshold. The interaction effect of threshold between stimulation mode and pulse shape was not significant ($p > 0.05$).

Due to concern about MALs that may have been underestimated for Tri stimulation, the ANOVA analysis was repeated and conducted separately for Mono and Tri stimulation. Results were similar as reported earlier. For both Mono and Tri stimulation, DP pulses led to significantly lower thresholds ($p < 0.05$) and did not lead to changes in MALs ($p > 0.05$). No significant difference was found across electrodes ($p > 0.05$).

Figure 3 shows the channel-to-channel variability across electrodes. This measure was derived by computing the mean of the unsigned difference between apical and middle electrode thresholds and the unsigned difference between middle and basal electrode thresholds (Pfingst & Xu 2004). Because the step sizes used for DP mode were eight times larger than the step size used for BP mode, separate analyses were performed for BP and DP modes. The larger step sizes used for DP mode may have resulted in artificially smaller or larger channel-to-channel variability depending on whether the step sizes were too large or too small, respectively, compared with the JND in intensity near threshold. Results of the Wilcoxon signed-rank test showed that threshold variability across electrodes was higher for Tri stimulation compared with Mono stimulation in BP mode ($p < 0.05$), consistent with previous studies (Bierer 2007). Typically, variation in nerve survival patterns along the cochlea is expected, and if Tri stimulation does result in more spatially selective excitation patterns than Mono stimulation, we would expect threshold variability to be higher, reflecting the variation in thresholds of the underlying population of auditory neurons. On the other hand, we would expect threshold variability to be lower for Mono stimulation, due to the large overlap in the population of auditory neurons stimulated across electrodes. No statistically significant difference was seen in threshold variability between Mono and Tri stimulation

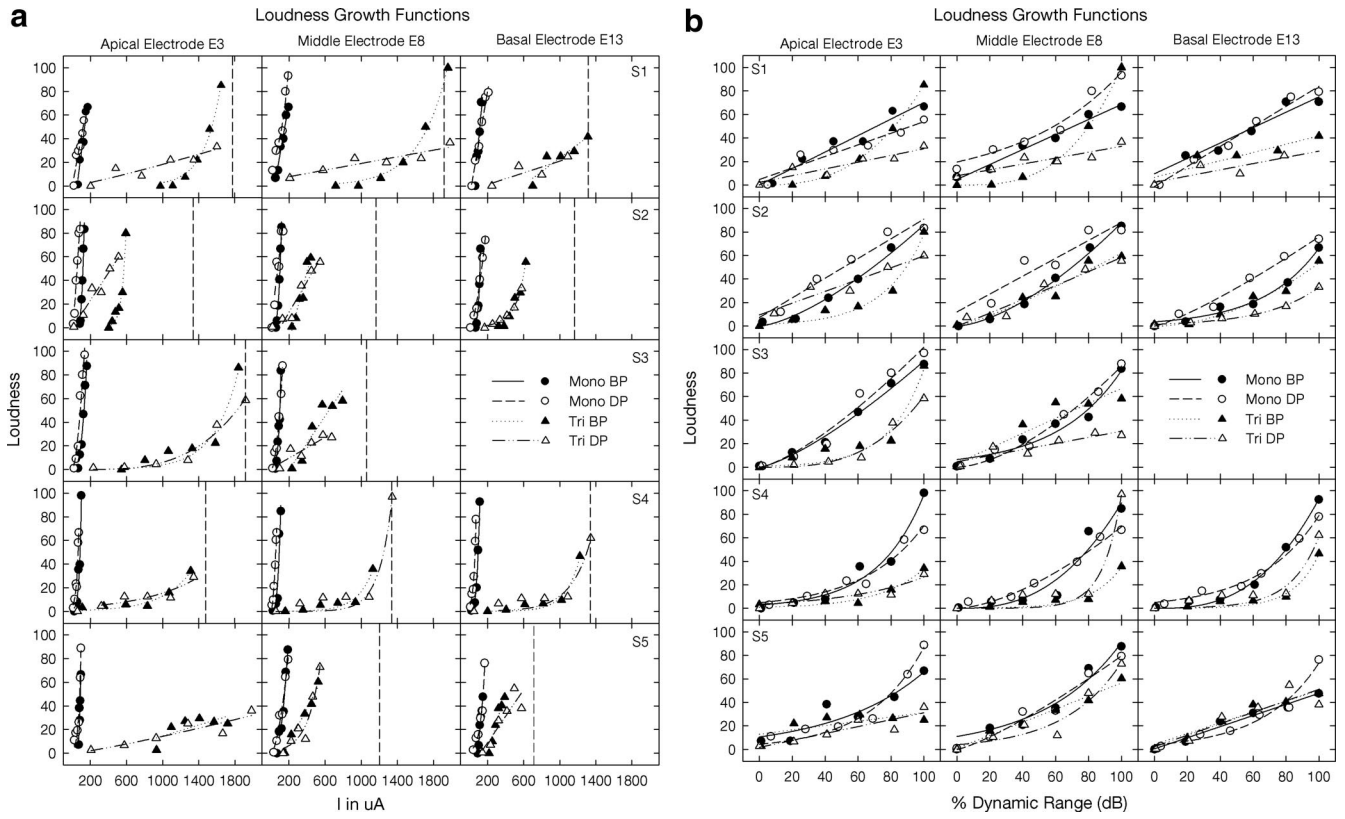

Fig. 4. Loudness growth functions for monopolar (circles, nondotted lines) versus tripolar (triangles, dotted lines) and biphasic (filled symbols, non-dashed lines) versus delayed pseudomonophasic (clear symbols, dashed lines) pulses across apical electrode E3, middle electrode E8, and basal electrode E13. Lines show best-fit curves from linear, exponential, or power functions. a, Loudness growth as a function of current amplitude in μA. Vertical dashed lines mark the compliance limit of the electrode tested. b, Loudness growth as a function of % dynamic range in dB.

in DP mode ($p > 0.05$), possibly due to the large step size in the adaptive procedure used to determine DP thresholds.

Experiment 2—Loudness Growth Functions

Because loudness growth in CI subjects is usually expansive (Chatterjee 1999; Chatterjee et al. 2000), shallower loudness growth may result in less compression required to restore normal loudness growth. The purpose of Experiment 2 was to determine whether loudness grows differently in different stimulus conditions.

Figure 4 shows loudness growth data from five subjects, with rows representing individual subjects and columns representing electrodes. The lines represent the best fit of the loudness growth data using one of the three models listed in Table 2. Figure 4a shows loudness estimates as a function of raw current amplitude in μA. The vertical line in each panel marks the compliance limit of the active electrode. As expected, due to differences in etiology and other audiological factors, there is great variability in loudness growth functions among CI subjects. In general, loudness growth functions were monotonic, except in a few cases where compliance limits might have caused loudness growth functions to plateau (e.g., S3 E8 Tri BP). The form of loudness growth functions also varied within subjects across different conditions (e.g., S1 E8). Figure 4b shows loudness estimates as a function of % dynamic range in dB. At MAL, the loudness estimates in Tri stimulation mode were lower than loudness estimates in Mono stimulation mode. It is possible that MALs for Tri stimulation were underestimated due to compliance limits of the CI device, because device compliance limits are often reached before MALs (Bierer 2007; Litvak et al. 2007). Although we have attempted to work around the device compliance limits increasing the pulse width and electrode spacing, subjects may have confused maximum loudness and annoyance, and may have labeled the stimuli as MAL when it was starting to be annoying, but not at equal loudness with other stimuli. The relationship between loudness and annoyance is complicated and may be influenced by the spectral character of the stimuli.

Figure 5 shows the average rates of loudness growth at 20, 40, 60, and 80% DR (dB) from five subjects. Data from three electrodes are plotted separately for clarity. In general, the slope of loudness growth function increased with percent dynamic range, indicating that the loudness growth function was on the average exponential.

Repeated measures ANOVA were used to evaluate loudness growth across different conditions with the following factors: baseline loudness (20, 40, 60, 80% DR dB), electrode (E3, E8, and E13), stimulation mode (Mono and Tri), and pulse shape (BP and DP). Dependent variables were loudness estimates and slopes of loudness growth functions on the best-fit curve. For the following statistical tests, two sets of ANOVA were performed due to missing data for S3's basal electrode—one with two electrodes and data from five subjects and another with three electrodes and data from four subjects.

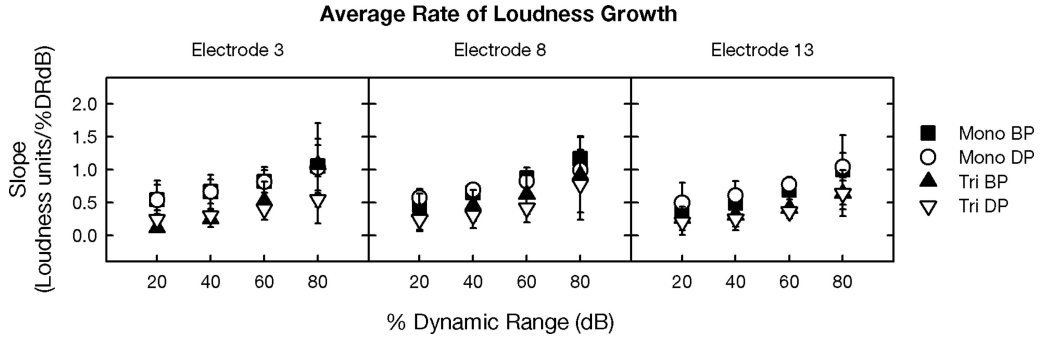

Fig. 5. Average rate of loudness growth for monopolar (squares and circles) versus tripolar (upright and inverted triangles) and biphasic (filled symbols) versus delayed pseudomonophasic (clear symbols) pulses across apical electrode E3, middle electrode E8, and basal electrode E13.

A significant difference was found in loudness estimates between Mono and Tri stimulation mode ($F[1,4] = 107$, $p < 0.01$; $F[1,3] = 19.4$, $p < 0.05$). The difference in slopes between Mono and Tri stimulation mode was also significant ($F[1,4] = 29.8$, $p < 0.01$; $F[1,3] = 36.0$, $p < 0.01$). No significant difference was found between BP and DP pulses ($p > 0.05$) or among different electrode positions ($p > 0.05$). The interaction between baseline loudness and pulse shape was not significant ($F[3,12] = 1.9$, $p > 0.05$; $F[3,9] = 0.95$, $p > 0.05$), indicating that the shapes of loudness growth function were similar for the two pulse waveforms and that loudness growth was not compromised by reduced thresholds and increased dynamic range for DP pulses.

Experiment 3—Just Noticeable Differences in Current Amplitude

Experiment 3 measured Weber fractions from JNDs in current amplitude in Mono and Tri stimulation as well as in BP and DP pulses. Preferably, similar shapes of loudness growth function despite reduced thresholds with DP pulses would be accompanied by at least equal, if not greater, number of steps for coding intensity compared with BP pulses.

Figure 6 shows Weber fractions in dB as a function of percent dynamic range in dB in three electrode positions (columns) from five subjects (top 5 rows) for four stimulation mode-pulse shape conditions: Mono (circles, solid lines) and Tri (triangles, dotted lines) modes, BP (filled symbols, non-dashed lines) and DP (clear symbols, dashed lines) pulses. Overall, Weber fractions decreased with percent dynamic range.

Weber fractions were fitted with the Weber function, where the slope a is the change in Weber fraction in dB per unit change in percent dynamic range in dB, and the sensitivity constant b is the Weber fraction at threshold. A large negative slope would indicate that Weber fraction improves rapidly as percent dynamic range increases, while a small negative slope would indicate that Weber fraction improves slowly. A large sensitivity constant would indicate that discrimination is poor at threshold and vice versa. An F-test was performed to determine whether or not slopes of fitted Weber functions were significantly different from zero. The p value indicated the probability that the negative slope was coincidentally due to random scatter of data.

The corresponding Weber function parameters a and b from five subjects are plotted in Figure 7 for different stimulation modes (circles or triangles) and pulse shapes (filled or clear). Black symbols in Figure 7 represent p values less than the significance level of 0.05, and gray symbols represent slopes that were not significantly different from 0. For most subjects,

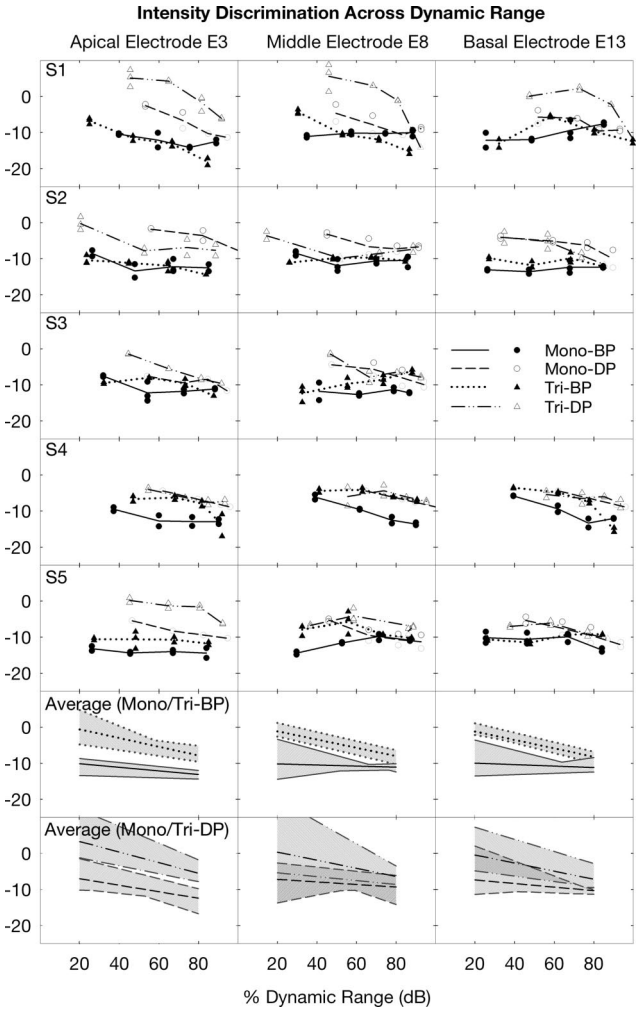

Fig. 6. Weber fractions in dB as a function of % dynamic range in dB for Mono-BP (filled circles), Mono-DP (clear circles), Tri-BP (filled triangles), and Tri-DP (clear triangles) stimuli across apical electrode E3, middle electrode E8, and basal electrode E13. Symbols represent individual data points and lines represent the mean. Gray symbols represent measurements that could not be obtained due to CI device resolution limits.

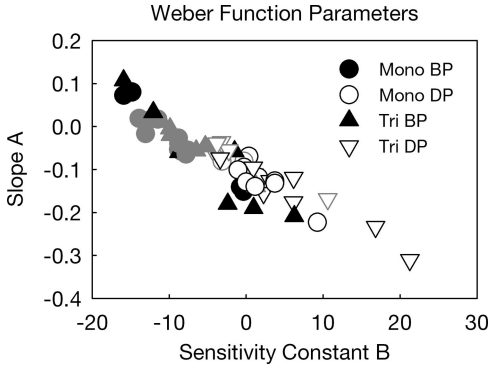

Fig. 7. Correlation between Weber parameters slope and sensitivity constant for Mono-BP (filled circles), Mono-DP (clear circles), Tri-BP (filled triangles), and Tri-DP (clear triangles). Filled and clear black symbols represent slopes significantly different from zero, and filled and clear gray symbols represent slopes not significantly different from zero.

slopes of Weber functions were negative and significantly different from zero. BP pulses (filled symbols) generally occupied the upper half and DP pulses (open symbols) occupied the lower half of Figure 7. This reflects the steeper slopes ($F[1,4] = 9.3$, $p < 0.05$; $F[1,3] = 3.7$, $p > 0.05$) and higher sensitivity constants ($F[1,4] = 21.0$, $p < 0.05$; $F[1,3] = 9.3$, $p > 0.05$) associated with DP pulses compared with BP pulses. These statistics were from two sets of repeated-measures ANOVA, with electrode, stimulation mode, and pulse shape as within-subject factors.

The bottom two rows in Figure 6 show the mean (black lines) and range (hatched areas outlined by gray lines) of fitted Weber function across five subjects for Mono-BP/Tri-BP (second to the last row) and Mono-DP/Tri-DP (last row). A slight decrease in slopes of Weber functions could also be seen across four stimulation mode-pulse shape combinations ($F[3,12] = 3.5$, $p < 0.05$; $F[3,9] = 2.3$, $p > 0.05$). The difference between electrodes was significant between E3 and E8 only, with E3 producing marginally larger sensitivity constants ($F[1,4] = 7.6$, $p = 0.05$) and steeper slopes ($F[1,4] = 16.8$, $p < 0.05$). Due to missing data for S3, these statistics were taken from two sets of repeated-measures ANOVA on Weber function parameters (slope a and sensitivity constant b) with two or three electrodes and four stimulation mode-pulse shape combinations as within-subject factors. Post hoc test results with Bonferroni correction showed that, on the average, the pair Mono-BP and Mono-DP produced statistically different sensitivity constants b for electrodes 3 and 8 ($p < 0.05$).

The number of discriminable steps is related to the Weber function slope a and sensitivity constant b. In general, across subjects and electrodes, shallower slopes ($r = 0.65$, $p < 0.01$) and smaller sensitivity constants ($r = -0.69$, $p < 0.01$) produced a greater number of discriminable steps, but the dynamic range did not correlate with the number of discriminable steps ($r = -0.16$, $p > 0.05$). Figure 8 shows the number of discriminable steps within the dynamic range, calculated from the fitted Weber functions. Again, due to missing data, two sets of repeated-measures ANOVA were performed on the number of discriminable steps. On average, the number of steps for coding intensity was similar across electrodes ($F[1,4] = 0.62$, $F[2,6] = 0.88$, $p > 0.05$). In general, the number of discriminable steps decreased from Mono-BP, Tri-BP, Tri-DP,

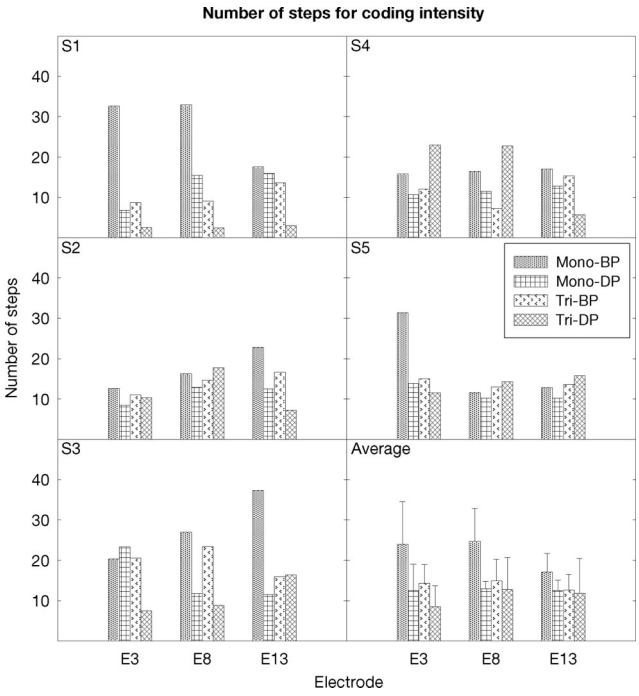

Fig. 8. Number of discriminable steps with Mono-BP (filled circles), Mono-DP (clear circles), Tri-BP (filled triangles), and Tri-DP (clear triangles) stimuli for apical electrode E3, middle electrode E8, and basal electrode E13.

to Mono-DP ($F[3,12] = 5.6$, $p < 0.05$; $F[1.5,9] = 4.4$, $p > 0.05$). For most subjects, the number of steps for DP pulses was generally near or below that of BP pulses for both Mono and Tri stimulation modes, consistent with the general trend. However, a few show deviations from the general trend (e.g., S4—E8 and E13). Overall, there was no statistical evidence that the number of discriminable steps is dependent on stimulation mode or pulse shape.

DISCUSSION

The main finding from this study is that DP pulses reduce thresholds and increase dynamic range for both Mono and Tri stimulation modes without compromising on the shape of loudness growth across its dynamic range. However, they produce larger intensity discrimination limens near thresholds than at higher current levels and slightly smaller number of discriminable steps compared with BP pulses. The following sections discuss possible physiological mechanisms contributing to observed results and possible implications of observed results in CI design and performance.

Detection Thresholds and MALs

Data from this study echoed results from previous studies that found lowered thresholds but relatively smaller changes in MALs for DP pulses using monopolar and bipolar stimulation (Carlyon et al. 2005; van Wieringen et al. 2005; Macherey et al. 2006), as well as results from previous studies that found a parallel increase in thresholds and MALs for Tri stimulation compared with Mono stimulation (Mens & Berenstein 2005; Litvak et al. 2007). The threshold drop in DP compared with BP pulses is mainly due to a delay in charge recovery of the

second phase that results in more efficient excitation (van den Honert & Mortimer 1979; van Wieringen et al. 2008). The threshold increase in Tri compared with Mono stimulation is due to the "shunt" produced by placing return electrodes adjacent to active electrodes in a highly conductive fluid, which increases the longitudinal lateral current flowing within the scala tympani and reduces the current flow through the cochlear wall (Kral et al. 1998), thereby exciting fewer number of neurons for a given stimulation level. On the other hand, MALs were relatively similar for DP and BP pulses, because the mechanisms that reduce threshold drops are not as effective at suprathreshold levels. Since loudness is related to integration of neural activity in the cochlea, thresholds and MALs are higher for more focused Tri stimulation compared with broader Mono stimulation (Chatterjee 1999; Bierer 2007).

Loudness Growth

Differences in dynamic range in terms of microamperes complicate direct comparisons of loudness growth functions (Fu 2005). To account for this, we plotted loudness growth as a function of percent dynamic range in dB. Because the shape of loudness growth depends on loudness models, the slope of loudness functions were evaluated at specific points within the dynamic range and compared across conditions and across subjects. We found no difference in slopes at different points along the dynamic range between BP and DP pulses, indicating that the shift in threshold and increase in dynamic range did not affect loudness growth. Since the dynamic range in μA was larger for DP than BP pulses, the same loudness growth as a function of percent dynamic range in dB implied that the spread of excitation and/or increase in discharge rate was less steep as a function of stimulus level for DP pulses. Compared with Mono stimulation, Tri stimulation produced shallower loudness growth as a function of percent dynamic range presumably due to MALs that may have been underestimated.

Previous studies may explain the results of the present study. For Tri stimulation, due to MALs that may have been underestimated, the results on loudness growth functions are not as clear, but animal studies have demonstrated decreased rates of neural recruitment in focused electrode configurations such as bipolar stimulation (Schindler et al. 1977; Black & Clark 1980; Marsh et al. 1981; van den Honert & Stypulkowski 1987) and tripolar stimulation (Bierer & Middlebrooks 2002; Bonham & Litvak 2008), especially in the lower part of the dynamic range. Using a model where loudness was proportional to total neuronal activity calculated from the spatial activation pattern, Goldwyn et al. (2010) also predicted that loudness growth with full tripolar stimulation would be shallower than monopolar or partial tripolar stimulation. Miller et al. (2003) observed a slowed growth in evoked compound action potentials when using focused stimulation modes and suggested a shift in site of excitation from peripheral to central processes as stimulus levels increase from low to high. Peripheral excitation decreases the rate of fiber recruitment due to the fanned-out geometry of the neurons at the periphery, while central excitation produces a higher number of fibers recruited for a given stimulus intensity due to the higher density of neurons at central sites (Marsh et al. 1981). For DP pulses, no previous physiological studies have been done, but the mechanism for a slowed loudness growth may be similar.

Intensity Discrimination

Our results are generally consistent with previous studies in electric hearing that used BP pulses (Nelson et al. 1996). Herein, the overall average normalized slope was -0.096 ± 0.10, comparable to those previously reported for BP pulses and within the range of acoustic hearing (-0.06 to -0.10). The overall average sensitivity constant was -2.6 ± 7.8, within the range reported in electric hearing (-0.43 to -20.40) and slightly better than that reported in acoustic hearing (0.60 to -3.34 dB). The number of discriminable steps ranged from 5.3 to 48.3, comparable to that reported in other electric hearing studies (6.6 to 45.2), but much smaller than 82.8 steps reported in acoustic hearing (Nelson et al. 1996).

In contrast to acoustic stimulation where increased spread of excitation produces smaller Weber fractions (Florentine & Buus 1981), Weber fractions in electric hearing seem to be similar for Mono and bipolar stimulation (Drennan & Pfingst 2005) or Mono and Tri stimulation (the present study). For DP pulses, Weber function slopes were significantly steeper and sensitivity constants were significantly higher compared with BP pulses. Higher sensitivity constants or larger discrimination limens at low stimulus levels and steeper slopes in Weber functions may reflect characteristics of peripheral stimulation (Nelson et al. 1996). In addition, for DP pulses, it may reflect increased internal noise levels possibly due to greater effect of noisy sodium channels during the interphase gap and the low-amplitude second phase. In the deafened ear, few peripheral processes are left intact (Fayad & Linthicum 2006; Nadol & Eddington 2006); but a small number of surviving processes could produce a difference in loudness coding (Viemeister 1988).

In general, the dynamic range did not correlate with the number of discriminable steps, consistent with previous studies (Kreft et al. 2004; Galvin & Fu 2009), which found that despite increased dynamic range with high stimulation rates, the number of discriminable steps remained constant. The number of discriminable steps also did not depend on stimulation mode or pulse shape. A similar finding was reported in a previous study that used a delayed charge recovery pulse shape (van Wieringen et al. 2006).

Zeng and Shannon (1999) demonstrated a clear inverse relationship between the size of JND and the slope of the loudness growth function in a group of Ineraid CI subjects. Galvin and Fu (2009) also found a correlation between loudness growth and the size of JND across different pulse rates in Nucleus users. In a group of Clarion users, the present results showed a similar relationship for BP pulses but not for DP pulses.

Effect of Stimulus Parameters

A 100 Hz stimulation rate was chosen in this study, as the effect of delaying charge recovery is greater at low stimulation rates (Carlyon et al. 2005). This 100 Hz rate is much lower than stimulation rates in current CIs, which range from 800 to 3000 pps per channel. For BP pulses, in general, as pulse rate decreases, threshold and MALs increase and net dynamic range decreases (Shannon 1985; Kreft et al. 2004; Galvin & Fu 2005; van Wieringen et al. 2006; Galvin & Fu 2009). Few studies have investigated the effect of pulse rate on DP pulses. In a study that used a similar delayed charge recovery pulse shape (van Wieringen et al. 2006), pulse rate did not affect dynamic

range; in addition, the threshold versus pulse rate function was found to be monotonic for BP but nonmonotonic for the delayed stimulus, with a peak in threshold between 400 and 1000 Hz.

The pulse duration was initially chosen to be 107.8 μsecs, slightly longer than values typically used in Clarion devices. Short pulse duration stimuli are more effective at delivering charge (Shannon 1985). We used a longer pulse duration because of compliance limits in the CI device but understand that pulse duration may also affect the present results. For example, longer phase duration was found to increase the rate of loudness growth in electric stimulation (Chatterjee et al. 2000). To fully understand the interactions between loudness and stimulus configuration, a more complete set of stimulus parameters needs to be investigated.

Relationship to CI Design and Performance

Intensity, especially changes in intensity over time, is a fundamental cue for speech perception. This section examines the role of intensity coding, including thresholds, dynamic range, loudness growth, and intensity discrimination in CI design and performance.

First, there is no evidence that speech perception is related to mean thresholds (Pfingst et al. 2004). While a reduced dynamic range has negligible effects on phoneme recognition in quiet, it may significantly reduce phoneme recognition in noise (Zeng & Galvin 1999). From this point of view, DP pulses have the potential to alleviate the decreased dynamic range problem associated with Tri stimulation.

Loudness growth, together with the dynamic range, determines the amount of amplitude compression required to restore normal loudness growth. Although the degree of compression has little effect on speech in quiet, best performance and listening comfort tend to be achieved with the type of compression that restores normal loudness growth (Fu & Shannon 1998). Theoretically, there exists a compression function that can restore normal loudness growth in any electric stimulation mode, including combined Tri and DP stimulation. However, the present finding of a similar loudness growth at suprathreshold levels between different stimulus conditions suggests little or no power savings for DP pulses.

Intensity resolution is an important contributor to speech perception (Rosen 1992). Intensity discrimination is closely related to modulation detection (Wojtczak & Viemeister 1999; Donaldson & Viemeister 2000), which plays an important role in speech recognition in CIs. Modulation detection has been correlated with speech performance (Cazals et al. 1994; Fu 2002).* Elevated modulation detection thresholds in focused stimulation modes such as bipolar stimulation compared with broad stimulation modes such as Mono stimulation could account for poor speech recognition performance (Middlebrooks 2008) observed in experimental speech processing strategies using Tri stimulation (Mens & Berenstein 2005). In the absence of modulation detection data using Tri stimulation and DP pulses, the present intensity discrimination data suggest that DP pulses may not improve speech perception by improving loudness cues in Tri stimulation. Power savings may also be limited. However, the use of DP pulses may still improve speech perception in other ways that have not been tested, such as improved spatial selectivity and reduced channel interaction.

*Cazals et al. (1994) correlated phonetic recognition with shapes of TMTF: Subjects with flat TMTFs had poorer speech recognition than subjects with band-pass TMTFs. However, the study did not control for loudness cues that subjects with flat TMTFs could have used to perform the modulation task (Donaldson & Viemeister 2002). On the other hand, Fu et al. (2002) correlated phonetic recognition with absolute modulation sensitivity at 100 Hz modulation frequency.

ACKNOWLEDGMENTS

The authors thank the subjects for their time and dedication. They also thank Dr. Leonid Litvak for information on compliance limits and technical support on Advanced Bionics BEDCS research interface.

This work was supported by the National Institutes of Health and Department of Health and Human Services (1R01-DC008858, 5RO1-DC007714, and P30-DC008369).

Address for correspondence: Tiffany Elise H. Chua, University of California, Irvine, 364 Med Surge II, Irvine, CA 92697. E-mail: tchua@uci.edu.

Received November 21, 2009; accepted March 10, 2011.

REFERENCES

Akaike, H. (1978). A Bayesian analysis of the minimum AIC procedure. *Ann Inst Stat Math*, *30*, 9–14.

Akaike, H. (1979). A Bayesian extension of the minimum AIC procedure of autoregressive model fitting. *Biometrika*, *66*, 237–242.

Bierer, J. A. (2007). Threshold and channel interaction in cochlear implant users: Evaluation of the tripolar electrode configuration. *J Acoust Soc Am*, *121*, 1642–1653.

Bierer, J. A., & Middlebrooks, J. C. (2002). Auditory cortical images of cochlear-implant stimuli: Dependence on electrode configuration. *J Neurophysiol*, *87*, 478–492.

Black, R. C., & Clark, G. M. (1980). Differential electrical excitation of the auditory nerve. *J Acoust Soc Am*, *67*, 868–874.

Bonham, B. H., & Litvak, L. M. (2008). Current focusing and steering: Modeling, physiology, and psychophysics. *Hear Res*, *6*, 6.

Bonnet, R. M., Frijns, J. H., Peeters, S., et al. (2004). Speech recognition with a cochlear implant using triphasic charge-balanced pulses. *Acta Otolaryngol*, *124*, 371–375.

Bozdogan, H. (1987). Model selection and Akaike's information criterion (AIC): The general theory and its analytical extensions. *Psychometrika*, *52*, 345–370.

Brummer, S. B., & Turner, M. J. (1977). Electrochemical considerations for safe electrical stimulation of the nervous system with platinum electrodes. *IEEE Trans Biomed Eng*, *24*, 59–63.

Burnham, K. P., & Anderson, D. R. (2002). Model Selection and Multimodel Inference: A Practical Information-Theoretic Approach. New York, NY: Springer Verlag.

Carlyon, R. P., van Wieringen, A., Deeks, J. M., et al. (2005). Effect of inter-phase gap on the sensitivity of cochlear implant users to electrical stimulation. *Hear Res*, *205*, 210–224.

Cazals, Y., Pelizzone, M., Saudan, O., et al. (1994). Low-pass filtering in amplitude modulation detection associated with vowel and consonant identification in subjects with cochlear implants. *J Acoust Soc Am*, *96*, 2048–2054.

Chatterjee, M. (1999). Effects of stimulation mode on threshold and loudness growth in multielectrode cochlear implants. *J Acoust Soc Am*, *105*, 850–860.

Chatterjee, M., Fu, Q. J., Shannon, R. V. (2000). Effects of phase duration and electrode separation on loudness growth in cochlear implant listeners. *J Acoust Soc Am*, *107*, 1637–1644.

Cogan, S. F. (2008). Neural stimulation and recording electrodes. *Annu Rev Biomed Eng*, *10*, 275–309.

Donaldson, G. S., & Viemeister, N. F. (2000). Intensity discrimination and detection of amplitude modulation in electric hearing. *J Acoust Soc Am*, *108*, 760–763.

Drennan, W. R., & Pfingst, B. E. (2005). Current-level discrimination using bipolar and monopolar electrode configurations in cochlear implants. *Hear Res*, *202*, 170–179.

Eddington, D. K., Tierney, J., Noel, V., et al. (2004). Speech processors for auditory prostheses. Ninth quarterly progress report, NIH contract N01-DC-2-1001.

Fayad, J. N., & Linthicum, F. H., Jr. (2006). Multichannel cochlear implants: Relation of histopathology to performance. *Laryngoscope*, *116*, 1310–1320.

Florentine, M., & Buus, S. (1981). An excitation-pattern model for intensity discrimination. *J Acoust Soc Am*, *70*, 1646–1654.

Frijns, J. H., de Snoo, S. L., ten Kate, J. H. (1996). Spatial selectivity in a rotationally symmetric model of the electrically stimulated cochlea. *Hear Res*, 95, 33–48.

Fu, Q. J. (2002). Temporal processing and speech recognition in cochlear implant users. *Neuroreport*, *13*, 1635–1639.

Fu, Q. J. (2005). Loudness growth in cochlear implants: Effect of stimulation rate and electrode configuration. *Hear Res*, *202*, 55–62.

Fu, Q. J., & Shannon, R. V. (1998). Effects of amplitude nonlinearity on phoneme recognition by cochlear implant users and normal-hearing listeners. *J Acoust Soc Am*, *104*, 2570–2577.

Galvin, J. J., & Fu, Q. J. (2005). Effects of stimulation rate, mode and level on modulation detection by cochlear implant users. *J Assoc Res Otolaryngol*, *6*, 269–279.

Galvin, J. J., & Fu, Q. J. (2009). Influence of stimulation rate and loudness growth on modulation detection and intensity discrimination in cochlear implant users. *Hear Res*, *250*, 46–54.

Goldwyn, J. H., Bierer, S. M., Bierer, J. A. (2010). Modeling the electrode-neuron interface of cochlear implants: Effects of neural survival, electrode placement, and the partial tripolar configuration. *Hear Res*, *268*, 93–104.

Grantham, D. W., & Yost, W. A. (1982). Measures of intensity discrimination. *J Acoust Soc Am*, *72*, 406–410.

Hong, R. S., Rubinstein, J. T., Wehner, D., et al. (2003). Dynamic range enhancement for cochlear implants. *Otol Neurotol*, *24*, 590–595.

Ifukube, T., & White, R. L. (1987). Current distributions produced inside and outside the cochlea from a scala tympani electrode array. *IEEE Trans Biomed Eng*, *34*, 883–890.

Jolly, C. N., Spelman, F. A., Clopton, B. M. (1996). Quadrupolar stimulation for Cochlear prostheses: Modeling and experimental data. *IEEE Trans Biomed Eng*, *43*, 857–865.

Kral, A., Hartmann, R., Mortazavi, D., et al. (1998). Spatial resolution of cochlear implants: The electrical field and excitation of auditory afferents. *Hear Res*, *121*, 11–28.

Kreft, H. A., Donaldson, G. S., Nelson, D. A. (2004). Effects of pulse rate and electrode array design on intensity discrimination in cochlear implant users. *J Acoust Soc Am*, *116*, 2258–2268.

Litvak, L. M., Spahr, A. J., Emadi, G. (2007). Loudness growth observed under partially tripolar stimulation: Model and data from cochlear implant listeners. *J Acoust Soc Am*, *122*, 967–981.

Macherey, O., van Wieringen, A., Carlyon, R. P., et al. (2006). Asymmetric pulses in cochlear implants: Effects of pulse shape, polarity, and rate. *J Assoc Res Otolaryngol*, *7*, 253–266.

Marsh, R. R., Yamane, H., Potsic, W. P. (1981). Effect of site of stimulation on the guinea pig's electrically evoked brain stem response. *Otolaryngol Head Neck Surg*, *89*, 125–130.

Mens, L. H., & Berenstein, C. K. (2005). Speech perception with mono- and quadrupolar electrode configurations: A crossover study. *Otol Neurotol*, *26*, 957–964.

Merrill, D. R., Bikson, M., Jefferys, J. G. R. (2005). Electrical stimulation of excitable tissue: Design of efficacious and safe protocols. *J Neurosci Methods*, *141*, 171–198.

Middlebrooks, J. C. (2008). Cochlear-implant high pulse rate and narrow electrode configuration impair transmission of temporal information to the auditory cortex. *J Neurophysiol*, *100*, 92–107.

Miller, C. A., Abbas, P. J., Nourski, K. V., et al. (2003). Electrode configuration influences action potential initiation site and ensemble stochastic response properties. *Hear Res*, *175*, 200–214.

Morse, R. P., Morse, P. F., Nunn, T. B., et al. (2007). The effect of Gaussian noise on the threshold, dynamic range, and loudness of analogue cochlear implant stimuli. *J Assoc Res Otolaryngol*, *8*, 42–53.

Nadol, J. B., Jr., & Eddington, D. K. (2006). Histopathology of the inner ear relevant to cochlear implantation. *Adv Otorhinolaryngol*, *64*, 31–49.

Nelson, D. A., Schmitz, J. L., Donaldson, G. S., et al. (1996). Intensity discrimination as a function of stimulus level with electric stimulation. *J Acoust Soc Am*, *100*, 2393–2414.

Pfingst, B. E., Burnett, P. A., Sutton, D. (1983). Intensity discrimination with cochlear implants. *J Acoust Soc Am*, *73*, 1283–1292.

Pfingst, B. E., & Xu, L. (2004). Across-site variation in detection thresholds and maximum comfortable loudness levels for cochlear implants. *J Assoc Res Otolaryngol*, *5*, 11–24.

Pfingst, B. E., Xu, L., Thompson, C. S. (2004). Across-site threshold variation in cochlear implants: Relation to speech recognition. *Audiol Neurotol*, *9*, 341–352.

Robblee, L. S., & Rose, T. L. (1990). Electrochemical Guidelines for Selection of Protocols and Electrode Materials for Neural Stimulation. In W. F. Agnew & D. B. McCreery (Eds). *Neural Prostheses: Fundamental Studies* (pp. 25–66). Englewood Cliffs, NJ: Prentice-Hall.

Rosen, S. (1992). Temporal information in speech: Acoustic, auditory and linguistic aspects. *Philos Trans R Soc Lond B Biol Sci*, *336*, 367–373.

Rubinstein, J. T., Wilson, B. S., Finley, C. C., et al. (1999). Pseudospontaneous activity: Stochastic independence of auditory nerve fibers with electrical stimulation. *Hear Res*, *127*, 108–118.

Schindler, R. A., Merzenich, M. M., White, M. W., et al. (1977). Multielectrode intracochlear implants. Nerve survival and stimulation patterns. *Arch Otolaryngol*, *103*, 691–699.

Shannon, R. V. (1985). Threshold and loudness functions for pulsatile stimulation of cochlear implants. *Hear Res*, *18*, 135–143.

Shepherd, R. K., & Javel, E. (1999). Electrical stimulation of the auditory nerve: II. Effect of stimulus waveshape on single fibre response properties. *Hear Res*, *130*, 171–188.

Snyder, R. L., Bierer, J. A., Middlebrooks, J. C. (2004). Topographic spread of inferior colliculus activation in response to acoustic and intracochlear electric stimulation. *J Assoc Res Otolaryngol*, *5*, 305–322.

Snyder, R. L., Middlebrooks, J. C., Bonham, B. H. (2008). Cochlear implant electrode configuration effects on activation threshold and tonotopic selectivity. *Hear Res*, *235*, 23–38.

van den Honert, C., & Mortimer, J. (1979). The response of the myelinated nerve fiber to short duration biphasic stimulating currents. *Ann Biomed Eng*, *7*, 117–125.

van den Honert, C., & Stypulkowski, P. H. (1987). Single fiber mapping of spatial excitation patterns in the electrically stimulated auditory nerve. *Hear Res*, *29*, 195–206.

van Wieringen, A., Carlyon, R. P., Laneau, J., et al. (2005). Effects of waveform shape on human sensitivity to electrical stimulation of the inner ear. *Hear Res*, *200*, 73–86.

van Wieringen, A., Carlyon, R. P., Macherey, O., et al. (2006). Effects of pulse rate on thresholds and loudness of biphasic and alternating monophasic pulse trains in electrical hearing. *Hear Res*, *220*, 49–60.

van Wieringen, A., Macherey, O., Carlyon, R. P., et al. (2008). Alternative pulse shapes in electrical hearing. *Hear Res*, *242*, 154–163.

Viemeister, N. F. (1988). Intensity coding and the dynamic range problem. *Hear Res*, *34*, 267–274.

Wagenmakers, E.-J., & Farrell, S. (2004). AIC model selection using Akaike weights. *Psychon Bull Rev*, *11*, 192–196.

Wojtczak, M., & Viemeister, N. F. (1999). Intensity discrimination and detection of amplitude modulation. *J Acoust Soc Am*, *106*, 1917–1924.

Zeng, F. G., Fu, Q. J., Morse, R. (2000). Human hearing enhanced by noise. *Brain Res*, *869*, 251–255.

Zeng, F. G., & Galvin, J. J. (1999). Amplitude mapping and phoneme recognition in cochlear implant listeners. *Ear Hear*, *20*, 60–74.

Zeng, F. G., & Shannon, R. V. (1999). Psychophysical laws revealed by electric hearing. *Neuroreport*, *10*, 1931–1935.